



# Rings and Chains: Synthesis and Characterization of Polyferrocenylmethylene

Tamara Winter, Wasim Haider, Alexander Schießler, Volker Presser, Markus Gallei,\* and André Schäfer\*

The synthesis and characterization of polyferrocenylmethylene (PFM) starting from dilithium 2,2-bis(cyclopentadienide)propane and a  $\text{Me}_2\text{C}[1]$ magnescenophane is reported. Molecular weights of up to  $M_w = 11\,700\text{ g mol}^{-1}$  featuring a dispersity,  $\mathcal{D}$ , of 1.40 can be achieved. The material is studied by different methods comprising nuclear magnetic resonance (NMR) spectroscopy, matrix-assisted laser desorption/ionization time of flight (MALDI-ToF) mass spectrometry, differential scanning calorimetry (DSC), and thermogravimetric analysis (TGA) measurements elucidating the molecular structure and thermal properties of these novel polymers. Moreover, cyclic voltammetry (CV) reveals quasi-reversible oxidation and reduction behavior and communication between the iron centers. Also, the crystal structure of a related cyclic hexamer is presented.

## 1. Introduction

In the recent past a unique class of smart and functional materials, so-called metallopolymers, centered scientific studies for a manifold of applications. The key features of these materials are their fascinating redox-responsive (opto)electronic as well as catalytic switching capabilities. Moreover, as part of more complex polymer architectures such as block copolymers or dendritic polymers also their excellent structure formation and separation characteristic have been shown.<sup>[1–8]</sup> Within this context, one of the most significant representative in this emerging field is the ferrocene/ferrocenium redox couple. The latter provides a highly revers-

ible (electro)chemical addressability between a rather hydrophobic ferrocene and a more hydrophilic ferrocenium ion.<sup>[9–13]</sup> In general, the incorporation of the transition metal into the polymer architecture can occur upon functionalization of the polymer backbone or the redox-active moiety can be laterally bonded to the polymer chains.

A fundamental breakthrough with respect to the synthesis of switchable ferrocene-containing main-chain polymers was the ring-opening polymerization (ROP) of strained metallocenophanes invented by Manners and co-workers.<sup>[2,4,14–16]</sup> On the other hand, also side-chain ferrocene-containing polymers attracted enormous attention for many interesting applications. Reviews in these fields are given by Zhou et al.,<sup>[2]</sup> the Tang's group,<sup>[17–19]</sup> and other authors.<sup>[20,21]</sup> Among such ferrocene-containing macromolecules, polyferrocenylsilanes are a very popular class of compounds.<sup>[4,22]</sup> They are generally prepared via ring-opening polymerization starting from the corresponding ring-strained Si[1]ferrocenophanes. Although this synthetic route facilitates diverse substituents on the silicon atom and can also be applied to some other ferrocenophanes, it does not allow for the synthesis of a methylene-bridged polyferrocenophane, since a C[1]ferrocenophane is unknown and believed to be unstable due to its large ring-strain.<sup>[23]</sup> To circumvent this difficulty, we explored using s-block metal-based precursors for transmetalation reactions since Cp-compounds of s-block metals are versatile Cp transfer reagents.

In this study, we synthesized polyferrocenylmethylene, 1, by transmetalation of dilithium 2,2-bis(cyclopentadienide)propane or  $\text{Me}_2\text{C}[1]$ magnescenophane with iron(II)-bromide and iron(II)-chloride. The obtained materials were fully

T. Winter  
Ernst-Berl-Institute of Chemical Engineering and Macromolecular Chemistry  
Technische Universität Darmstadt  
Alarich-Weiss-Straße 4, Darmstadt 64287, Germany  
T. Winter, W. Haider, Prof. M. Gallei, Dr. A. Schäfer  
Department of Chemistry  
Saarland University  
Saarbrücken 66123, Germany  
E-mail: markus.gallei@uni-saarland.de; andre.schaefer@uni-saarland.de

T. Winter, Prof. V. Presser  
Department of Materials Science and Engineering  
Saarland University  
Campus D2 2, Saarbrücken 66123, Germany

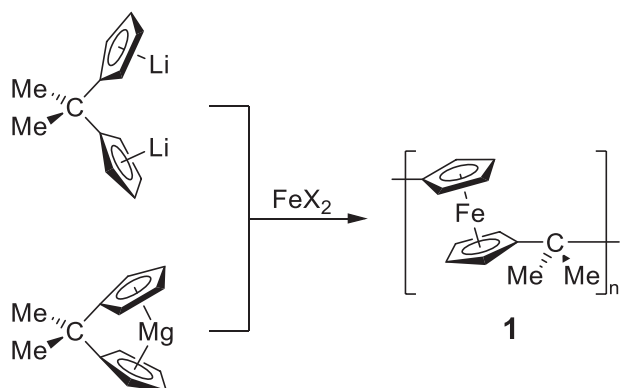
Dr. A. Schießler  
Mass Spectrometry, Department of Chemistry  
Technische Universität Darmstadt  
Alarich-Weiss-Straße 4, Darmstadt 64287, Germany

Prof. V. Presser  
INM – Leibniz-Institute for New Materials  
Campus D2 2, Saarbrücken 66123, Germany

The ORCID identification number(s) for the author(s) of this article can be found under <https://doi.org/10.1002/marc.202000738>.

© 2021 The Authors. Macromolecular Rapid Communications published by Wiley-VCH GmbH. This is an open access article under the terms of the Creative Commons Attribution License, which permits use, distribution and reproduction in any medium, provided the original work is properly cited.

DOI: 10.1002/marc.202000738



**Scheme 1.** Synthetic routes for the preparation of polyferrocenylmethylene (PFM) **1** (X = Cl and Br).

characterized by nuclear magnetic resonance (NMR) spectroscopy, size exclusion chromatography (SEC), multi-angle light scattering detection (MALLS), thermogravimetric analysis (TGA), differential scanning calorimetry (DSC), X-ray diffraction (XRD), and cyclic voltammetry (CV).

## 2. Results and Discussion

The synthesis of polyferrocenylmethylene (PFM) **1** was carried out via two different routes, starting either from a C[1]magnescenophane or the dilithiated 2,2-bis(cyclopentadienide)propane analog and iron(II)-chloride and iron(II)-bromide (**Scheme 1**).

The reaction was carried out at room temperature to give PFM **1** as a yellow and air-stable solid after workup. The product was soluble in THF and chloroform and insoluble in water, similar to polyferrocenylsilanes. The  $^1\text{H-NMR}$  spectrum exhibits two signals at  $\delta\ ^1\text{H} = 1.74$  and  $4.12$  ppm corresponding to the methyl groups and Cp protons, respectively, the latter coinciding with a singlet, similar to what has been observed for the silicon analog poly(ferrocenyldimethylsilane), PFS.<sup>[14]</sup>

**Table 1.** Molar masses and dispersity indices of the synthesized polyferrocenylmethylenes using different cyclopentadienide and iron precursors.

	Precursor	$\text{FeX}_2$	$M_n^a$ [g mol $^{-1}$ ]	$M_w^a$ [g mol $^{-1}$ ]	$\mathcal{D}$
1	$\text{Me}_2\text{C}[1]\text{Cp}_2\text{Li}_2$	$\text{FeCl}_2$	2200	3000	1.36
2	$\text{Me}_2\text{C}[1]\text{Cp}_2\text{Li}_2$	$\text{FeBr}_2$	2400	3400	1.37
3	$\text{Me}_2\text{C}[1]\text{Cp}_2\text{Mg}$	$\text{FeCl}_2$	4300	9000	2.09
4	$\text{Me}_2\text{C}[1]\text{Cp}_2\text{Mg}$	$\text{FeBr}_2$	8300	11 700	1.40

<sup>a</sup>)Determined by size exclusion chromatography in THF versus polystyrene standards.

The  $^{13}\text{C-NMR}$  spectrum shows two resonances for the aliphatic carbon atoms at  $\delta\ ^{13}\text{C} = 30.7$  and  $33.5$  ppm, and three resonances at  $\delta\ ^{13}\text{C} = 66.4$ ,  $67.7$ , and  $101.2$  ppm corresponding to the aromatic carbon atoms of the Cp groups.

The materials were additionally characterized by size exclusion chromatography (SEC) in THF versus PS standards. The corresponding molecular weight distribution is given in **Figure 1**, and the obtained data for all samples are compiled in **Table 1**. From the SEC measurements, it can be concluded that a polyferrocenylmethylene was achieved. Based on both applied synthetic protocols, differences in the obtained molar masses were observed; that is, the cyclopentadiene precursor has a significant influence on the resulting polymers' molecular weight. While the usage of dilithium 2,2-bis(cyclopentadienide) propane lead to molar masses around  $2200\ \text{g mol}^{-1}$  the corresponding C[1]magnescenophane yielded higher molar masses in the range of  $4000\text{--}8000\ \text{g mol}^{-1}$  (vs. PS as standard). Comparing the synthesis of batch three and four, as the only difference between both is the usage of the iron precursor, we see that using  $\text{FeBr}_2$  leads to a lower dispersity of PFM, indicating better control over the reaction.

The molar mass distribution of polymers derived via the  $\text{Me}_2\text{C}[1]\text{Cp}_2\text{Mg} + \text{FeCl}_2$  route revealed a more pronounced second molar mass distribution shifted to lower molar masses. This might result from different mechanisms, which, in the

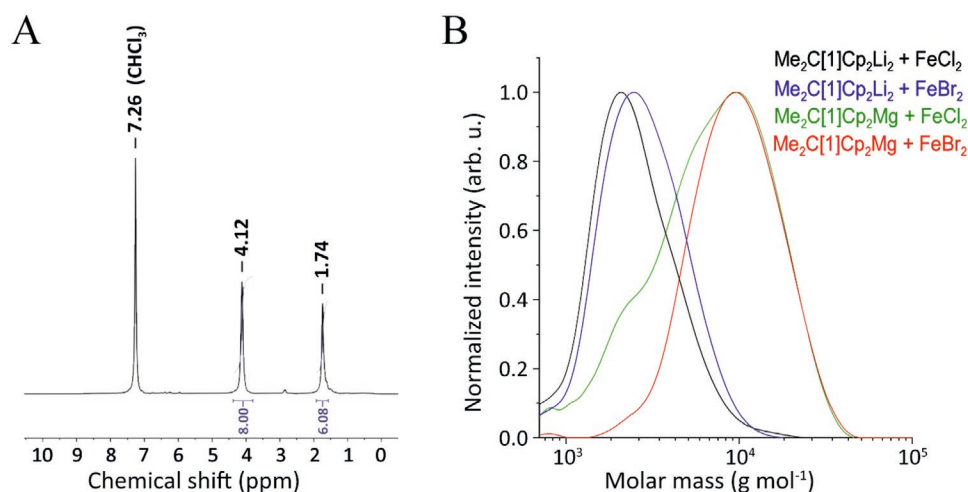


**Figure 1.** A)  $^1\text{H-NMR}$  spectrum of PFM, **1**, in  $\text{CDCl}_3$ ; B) Molar mass distribution obtained by size exclusion chromatography (SEC) in THF versus PS standards using different precursors:  $\text{Me}_2\text{C}[1]\text{Cp}_2\text{Li}_2 + \text{FeCl}_2$  (black line),  $\text{Me}_2\text{C}[1]\text{Cp}_2\text{Li}_2 + \text{FeBr}_2$  (blue line),  $\text{Me}_2\text{C}[1]\text{Cp}_2\text{Mg} + \text{FeCl}_2$  (green line) and  $\text{Me}_2\text{C}[1]\text{Cp}_2\text{Mg} + \text{FeBr}_2$  (red line).

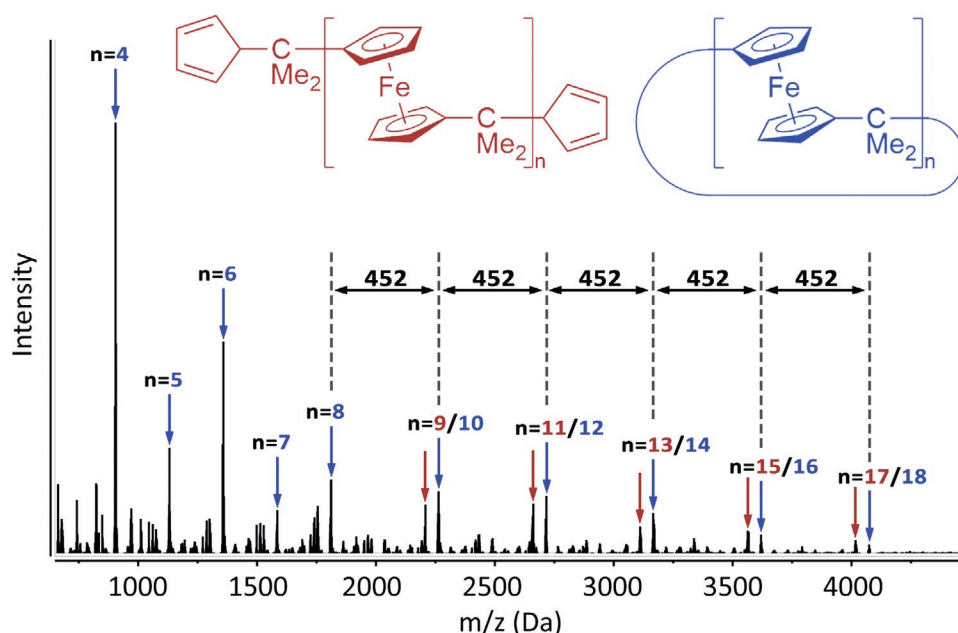


**Figure 2.** MALDI-ToF mass spectrum of PFM, 1, corresponding to batch No. 3 ( $\text{Me}_2\text{C}[\text{I}]\text{Cp}_2\text{Mg} + \text{FeCl}_2$  reaction) (repeat unit: 226 Da).

lithium precursor, promote backbiting and give cyclic oligomers rather than long-chain polymers.

In summary, the molar masses' resulting data vary between 2200–8300  $\text{g mol}^{-1}$ , and the dispersity,  $\mathcal{D}$ , was determined to be in a range of 1.36–2.09. Overall, the reaction of  $\text{Me}_2\text{C}[\text{I}]\text{magnesenocenophane}$  with iron(II)-bromide gave PFM with the highest molar masses ( $M_n = 8300$ ;  $M_w = 11700$ ). In general, apparent molar masses for metallopolymers by relative methods can strongly deviate from their absolute molar masses.<sup>[24–26]</sup> We also expect a difference in the hydrodynamic volume of PFM in THF compared to the values obtained for PS standards. For this purpose, the obtained PFM from the  $\text{Me}_2\text{C}[\text{I}]\text{Cp}_2\text{Mg} + \text{FeBr}_2$  reaction was additionally analyzed via SEC MALLS to gain more insights into the absolute molar mass. A corresponding molar mass of  $M_w = 13\,100 \text{ g mol}^{-1}$  was obtained. Therefore, it can be concluded that the hydrodynamic volumes of the samples and the PS standards are quite similar, and the SEC measurements are in good agreement.

To further investigate the molecular structure of PFM 1, we performed MALDI-ToF mass spectroscopy. The MALDI-ToF spectrum shows two different domains of cyclic and non-cyclic oligomers, with mass differences of two times the repeating unit (Figure 2).

The material contains at least some cyclic compounds besides the expected linear PFM chains. By extracting 1 with hexane, we separated a batch from which we could grow single crystals suitable for X-ray diffraction analysis. The resulting crystal structure indicates a cyclic hexamer (Figure 3), which has also been observed in the corresponding MALDI-ToF mass spectrum before.

The bonding situation of the ferrocene units in this hexameric macrocycle resembles unsubstituted ferrocene,<sup>[27–29]</sup> with  $\text{Fe-Cp}^{\text{cent}}$  bond lengths of 165.5 pm,  $\text{Fe-C}^{\text{Cp}}$  bond length of 204.5–207.2 pm, and a  $\text{Cp}^{\text{cent}}\text{-Fe-Cp}^{\text{cent}}$  angle of  $178.1^\circ$ . A hexameric macrocycle of ferrocene moieties directly linked together

has been reported by Albrecht and Long *et al.* in 2016 and shares similar bonding properties.<sup>[30]</sup>

Moreover, metal-containing polymers can be used as pre-ceramic materials, paving the way for a manifold of applications.<sup>[31–33]</sup> Thus, the herein presented iron-containing polymers were further analyzed regarding their thermal properties and the residues after ceramization by thermogravimetric analysis (TGA) and differential scanning calorimetry (DSC). The corresponding TGA curves of the PFM under synthetic air (10%  $\text{O}_2$  and 90%  $\text{N}_2$ ) and under a nitrogen atmosphere in a temperature range of 30 to 600  $^\circ\text{C}$  and the DSC thermogram are given in Figure S1 (Supporting Information). As seen from the

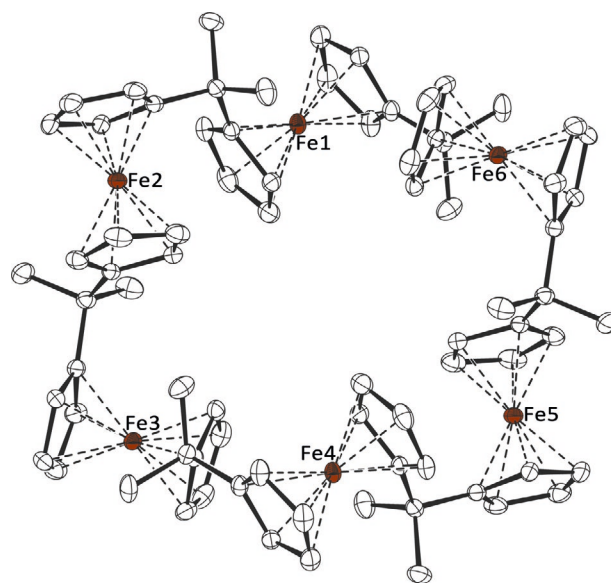


**Figure 3.** Cyclic hexamer of PFM in the crystal (displacement ellipsoids at 50% probability level; hydrogen atoms omitted for clarity).

thermogram, PFM shows a different thermal behavior under both conditions up to 300 °C. While treating the sample in synthetic air, the mass starts to increase at a temperature of 195 °C with a maximum of 250 °C and a total increase of 3 wt%. This feature is absent when using a nitrogen atmosphere. Also, the TGA curves revealed a different onset temperature regarding weight loss.

In the presence of oxygen, degradation starts at around 285 °C and at 350 °C in a nitrogen atmosphere (340 °C). In nitrogen, we also see a more distinct weight loss of up to 460 °C. At the end of the measurement, no further decomposition was observed, and the residual weight reached a constant value at higher temperatures for the synthetic air (410 °C) and the sample treated in a nitrogen atmosphere (480 °C).

A relatively high ceramic yield (compared to other linear ferrocene-containing polymers) was obtained under both conditions,<sup>[38-40]</sup> resulting in a final residue of ≈29 wt% (N<sub>2</sub>) and 35 wt% (synthetic air). While the oxygen treated sample changed from an initial orange to a more red-brownish powder, the sample treated under a nitrogen atmosphere presents a black material, presumably due to carbon. Both samples showed a magnetic response, as demonstrated by tracking the obtained powder with a magnet.

To give more insights into these materials' chemical structure and composition, X-ray diffraction (XRD) measurements of the obtained residues were carried out after thermal treatment (Figure S2, Supporting Information). The XRD pattern of the oxygen treated sample indicates the transformation into  $\alpha$ -Fe<sub>2</sub>O<sub>3</sub> (hematite), showing a trigonal crystal system with a corresponding *R* $\bar{3}$ *c* space group and lattice parameters of *a* = 5.03 Å and *c* = 13.74 Å. Compared to this, the samples treated under a nitrogen atmosphere leads to a combination of elemental iron (sharp reflections at 45°, 65°, and 82° 2 $\theta$ ) and iron carbide. Besides the TGA, the pristine polymer's DSC thermogram revealed a glass transition temperature (*T*<sub>g</sub>) at 60.5 °C.

In previous studies on different PFS structures, the Manners group showed that the *T*<sub>g</sub> of the corresponding polymer depends on the appropriate substituents located at the silicon atom in the polymer main chain.<sup>[22]</sup> They demonstrated in detail that a relatively high *T*<sub>g</sub> (above room temperature) is observed for methyl substituents due to the ferrocene moieties' static behavior or rather the cyclopentadiene rings. Compared to these findings, the obtained glass transition temperature of the herein presented polyferrocenylmethylene is in good agreement with expectations.

The metal atom within the PFM structure renders these materials to a functional material with redox-mediated switching capabilities. Therefore, the redox-responsiveness of the herein synthesized materials was investigated by electrochemical means. For this purpose, the mixture containing linear polymer chains of PFM as well as cyclic components were analyzed by cyclic voltammetry (CV) measurements using a 0.1 M solution of tetrabutylammonium hexafluorophosphate as the electrolyte in either acetonitrile (ACN) or THF in the potential range of -0.1 to +1.3 V versus Ag/Ag<sup>+</sup> were applied for scan rates of 25–50 mV s<sup>-1</sup>. The corresponding cyclic voltammograms are given in Figure 4.

The electrochemical studies revealed two quasi-reversible oxidation and reduction peaks, which was intensively studied

for other ferrocene-containing main-chain polymers as well as for cyclic ferrocene-containing molecules.<sup>[30,34]</sup> The presence of a two-electron transfer is based on the polymer chains' configuration and the location of the ferrocene groups themselves. Due to the small spacing between the individual ferrocene moieties, they can communicate with one another. In this regard, the first sequential oxidation of alternating iron sites along the polymer chains is observed, followed by the further oxidation of the remaining iron centers, where a higher potential need to be applied. The CVs in acetonitrile indicate polymer decomposition during cycling, as evidenced by a decreasing redox reaction intensity. This can be attributed to the sample preparation, where the PFM is first solved in THF and subsequently drop casted on the carbon electrode's surface. Consequently, the PFM loses adhesion during the measurement and is not connected to the current collector anymore, resulting in a smaller amount of material that can be electrochemically addressed. Moreover, the redox peaks' asymmetrical appearance, especially the high contrast in intensity according to the first oxidation peak, can also be affected by the solvent because acetonitrile acts as an electron donor.

Cyclic voltammetry data in TBAP/THF further confirm these results, leading to a significant enhancement according to the stability of the reaction, higher redox reversibility within ten cycles showing two oxidation peaks at 0.23 and 0.43 V as well as two reduction peaks at 0.31 and 0.11 V. Comparing different scan rates it can be further investigated that a slower scan rate can achieve a more uniform process. The corresponding peak separation of the alternating redox peaks represents the electronic interaction between the ferrocene compounds' iron centers within the polymer backbone. A higher peak separation,  $\Delta E_{1,2}$ , correlates with stronger internal communication and interactions between the individual ferrocene moieties. For example, the peak separation of biferrocene is 340 and 200 mV for [Fe( $\eta$ -C<sub>5</sub>-H<sub>4</sub>)<sub>2</sub>SiMe<sub>2</sub>]<sub>n</sub>. Therefore, we can demonstrate that the herein synthesized PFM shows a relatively high interaction with a peak separation of  $\Delta E_{1,2} = 200$  mV.<sup>[35,36]</sup>

In conclusion, an efficient protocol for the preparation of polyferrocenylmethylene (PFM), 1, is reported, which was previously unknown and cannot be obtained by simple ring-opening polymerization from a ferrocenophane. The material was characterized by NMR, SEC, SEC-MALLS, TGA, DSC, XRD, and MALDI-ToF MS, and its redox properties were investigated by CV measurements.

### 3. Experimental Section

NMR spectra were recorded on a Bruker Avance III 400 spectrometer and referenced by using the solvent signals.<sup>[37]</sup> Elemental analysis was performed on an Elementaranalysator vario MICRO cube. Single crystal X-ray diffraction analysis was carried out at low temperatures on a Bruker AXS D8 Venture diffractometer. Structure solution and refinement were performed using SHELX.<sup>[38]</sup>

Cyclic voltammetry (CV) measurements were carried out on a EmStat3+ potentiostat (Belltec) using PSTrace 5.5 as software to collect the data. All measurements were acquired using an Ag/Ag<sup>+</sup> reference electrode, a platinum counter electrode, and a glassy carbon working electrode with an inner diameter of 5 mm. The scan rate was varied at 25–50 mV s<sup>-1</sup> in a range of -0.1 to +1.3 V for oxidation and reduction experiments and calibrated versus ferrocene. For CV measurements,

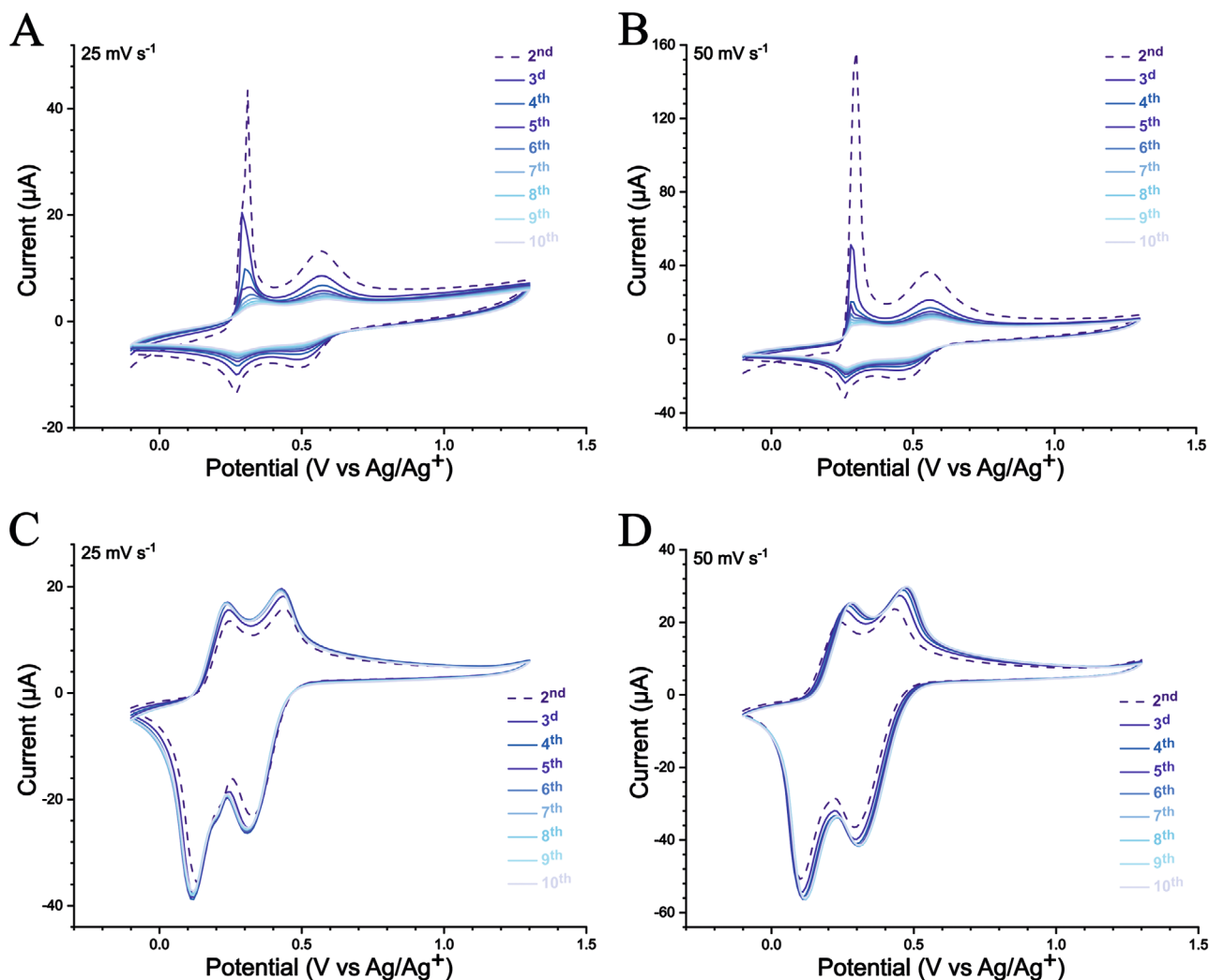


**Figure 4.** Cyclic voltammograms of polyferrocenylmethylene (PFM) in a potential range of  $-0.1$  to  $+1.3$  V versus  $\text{Ag}/\text{Ag}^+$  using tetrabutylammonium hexafluorophosphate in A, B: acetonitrile and C, D: tetrahydrofuran. The scan rate is given within the cyclic voltammogram.

a five-necked round-bottom flask was used with a solution of tetra *n*-butyl ammonium hexafluorophosphate ( $(n\text{Bu}_4\text{N})\text{PF}_6$ ) (0.1 M) in degassed tetrahydrofuran or acetonitrile as an electrolyte. Matrix-assisted laser desorption/ionization (MALDI) spectra were recorded with a Bruker Daltonik Autoflex speed TOF/TOF. The analyzer was a time-of-flight mass spectrometer. For the matrix the nonpolar, aprotic 2-[(2E)-3-(4-*tert*-butylphenyl)-2-methylprop-2-enylidene]malononitrile (DCTB) and  $\text{AgTFA}$  were used.

For evaluating the thermal properties, thermogravimetric analysis (TGA) was applied by using a Netzsch TGA 209 F1 Libra with a heating rate of  $20 \text{ K min}^{-1}$  in a range of  $30$ – $600$  °C in nitrogen or synthetic air (10%  $\text{O}_2$  and 90%  $\text{N}_2$ ) atmosphere. Differential scanning calorimetry (DSC) measurements were carried out with a Netzsch Polyma DSC 214 from  $-160$  to  $+300$  °C.

Standard size exclusion chromatography (SEC) was performed with a system composed of a 1260 Infinity II (Agilent Technologies), a 1260 VW detector (G7114A) at 260 nm (Agilent Technologies), and a 1260 RI detector (G7162A) at 35 °C (Agilent Technologies), THF as the mobile phase (flow rate  $1 \text{ mL min}^{-1}$ ) on a SDV column set from polymer standard service (PSS) (SDV  $10^3$  Å, SDV  $10^5$  Å, and SDV  $10^6$  Å). Calibration was carried out using PS standards from PSS. X-ray diffraction of the final residues after the thermogravimetric analysis was acquired with a D8 Discover diffractometer (Bruker AXS) using a copper

source (Cu- $\text{K}\alpha$ , 40 kV, 40 mA), a Göbel mirror, and a 0.5 mm point focus. Data were collected with a 2D VANTEC-500 detector covering an angle range of  $20^\circ$   $2\theta$ . Four frames were recorded at  $2\theta$  positions of  $20^\circ$ ,  $40^\circ$ ,  $60^\circ$ , and  $80^\circ$  using a measurement time of 2500 s for each frame.  $\text{Me}_2\text{C}[\text{I}]$ magnescenophane and dilithium 2,2-bis(cyclopentadienide) propane were prepared according to literature known routes.<sup>[39,40]</sup>

**Synthesis of Polyferrocenylmethylene (PFM) 1:** The synthesis was carried out under an argon 5.0 inert gas atmosphere using dry solvent.

**Method A:** Dilithium 2,2-bis(cyclopentadienide)propane ( $\text{Me}_2\text{C}[\text{I}]\text{Cp}_2\text{Li}_2$ ) (1.0 g, 5.43 mmol) and iron(II)-chloride (0.7 g, 5.43 mmol) or iron(II)-bromide (1.2 g, 5.43 mmol) were charged into a Schlenk flask. 100 mL of THF were added, and the resulting mixture was stirred overnight under an inert gas atmosphere at ambient temperature, turning from yellow to red/brown. Subsequently, the reaction mixture was poured into 200 mL of an ice-cold hexane/methanol/water mixture (10:9:1 by volume), resulting in the precipitation of the product collected by filtration, washed several times with water, and vacuum-dried. The material was diluted with THF, and all insoluble components were separated by filtration. The addition of hexane again precipitated the product. After drying in vacuum at 80 °C for 3 h a pale-yellow powder was observed (Yield: from  $\text{FeCl}_2$ : 12 mg; from  $\text{FeBr}_2$ : 115 mg).

**Method B:**  $\text{Me}_2\text{C}[\text{I}]\text{Magnescenophane}$  ( $\text{Me}_2\text{C}[\text{I}]\text{Cp}_2\text{Mg}$ ) (1.5 g, 7.88 mmol / 0.9 g, 4.63 mmol) and iron(II)-chloride (1.0 g, 7.88 mmol)

or iron(II)-bromide (1.0 g, 4.63 mmol) were charged into a Schlenk flask. 100 mL of THF were added, and the resulting mixture was stirred overnight under an inert gas atmosphere at ambient temperature, turning from yellow to red/brown. Isolation and workup were identical to what is described in Method A (Yield: from FeCl<sub>2</sub>: 100 mg; from FeBr<sub>2</sub>: 396 mg).

Elemental analysis for C<sub>13</sub>H<sub>14</sub>Fe: calculated: 69.06 at% C, 6.24 at% H; found: 66.18 at% C 6.09 at% H (low-carbon values were repeatedly and reproducibly observed upon analysis of different samples and have been described before in case of polyferrocenylsilanes.<sup>[41,42]</sup>)

<sup>1</sup>H NMR (400.13 MHz, CDCl<sub>3</sub>, δ): 4.12 (br s, 8H, Cp-H), 1.74 (br s, 6H, CH<sub>3</sub>).

<sup>13</sup>C NMR (100.62 MHz, CDCl<sub>3</sub>, δ): 101.2 (Cp), 67.7(Cp), 66.4 (Cp), 33.5 (C(CH<sub>3</sub>)<sub>2</sub>), 30.7 (C(CH<sub>3</sub>)<sub>2</sub>).

## Supporting Information

Supporting Information is available from the Wiley Online Library or from the author.

## Acknowledgements

T.W. and W.H. contributed equally to this work. The authors thank Lea Gemmer for TGA and DSC measurements and Blandine Bosmann for SEC measurements. Funding by the Deutsche Forschungsgemeinschaft (Emmy Noether Program, SCHA1915/3-1; INST 163/445-1 FUGG) and the Fonds der Chemischen Industrie is gratefully acknowledged. The INM authors thank Eduard Arzt for his continued support.

Open access funding enabled and organized by Projekt DEAL.

## Conflict of Interest

The authors declare no conflict of interest.

## Data Availability Statement

Research data are not shared.

## Keywords

electrochemistry, functional materials, metal-containing polymers, polyferrocenes, polymer synthesis

Received: December 16, 2020

Revised: January 20, 2021

Published online: February 7, 2021

- [1] M. Hadadpour, J. Gwyther, I. Manners, P. J. Ragogna, *Chem. Mater.* **2015**, *27*, 3430.
- [2] J. Zhou, G. R. Whittell, I. Manners, *Macromolecules* **2014**, *47*, 3529.
- [3] H. Gu, R. Ciganda, R. Hernandez, P. Castel, P. Zhao, J. Ruiz, D. Astruc, *Macromolecules* **2015**, *48*, 6071.
- [4] V. Bellas, M. Rehahn, *Angew. Chem., Int. Ed.* **2007**, *46*, 5082.
- [5] C. Rüttiger, H. Hübner, S. Schöttner, T. Winter, B. Kuttich, B. Stühn, M. Gallei, *ACS Appl. Mater. Interfaces* **2018**, *10*, 4018.
- [6] M. Gallei, C. Rüttiger, *Chem. - Eur. J.* **2018**, *24*, 10006.
- [7] L. Zhao, X. Liu, L. Zhang, G. Qiu, D. Astruc, H. Gu, *Coord. Chem. Rev.* **2017**, *337*, 4.

- [8] X. Su, K.-J. Tan, J. Elbert, C. Rüttiger, M. Gallei, T. F. Jamison, T. A. Hatton, *Energy Environ. Sci.* **2017**, *10*, 1272.
- [9] X. Feng, X. Sui, M. A. Hempenius, G. J. Vancso, *J. Am. Chem. Soc.* **2014**, *136*, 7865.
- [10] D. Scheid, C. Lederle, S. Vowinkel, C. G. Schäfer, B. Stühn, M. Gallei, *J. Mater. Chem. C* **2014**, *2*, 2583.
- [11] B. V. K. J. Schmidt, J. Elbert, C. Barner-Kowollik, M. Gallei, *Macromol. Rapid Commun.* **2014**, *35*, 708.
- [12] J. Song, D. Jańczewski, Y. Ma, L. van Ingen, C. E.e Sim, Q. Goh, J. Xu, G. J. Vancso, *Eur. Polym. J.* **2013**, *49*, 2477.
- [13] J. Elbert, M. Gallei, C. Rüttiger, A. Brunsen, H. Didzoleit, B. Stühn, M. Rehahn, *Organometallics* **2013**, *32*, 5873.
- [14] D. A. Foucher, B.-Z. Tang, I. Manners, *J. Am. Chem. Soc.* **1992**, *114*, 6246.
- [15] I. Manners, *Can. J. Chem.* **1998**, *76*, 371.
- [16] A. D. Russell, R. A. Musgrave, L. K. Stoll, P. Choi, H. Qiu, I. Manners, *J. Organomet. Chem.* **2015**, *784*, 24.
- [17] C. G. Hardy, L. Ren, J. Zhang, C. Tang, *Isr. J. Chem.* **2012**, *52*, 230.
- [18] Y. Yan, J. Zhang, L. Ren, C. Tang, *Chem. Soc. Rev.* **2016**, *45*, 5232.
- [19] C. G. Hardy, J. Zhang, Y. Yan, L. Ren, C. Tang, *Prog. Polym. Sci.* **2014**, *39*, 1742.
- [20] R. Pietschnig, *Chem. Soc. Rev.* **2016**, *45*, 5216.
- [21] M. Gallei, *Macromol. Chem. Phys.* **2014**, *215*, 699.
- [22] R. L. Hailes, A. M. Oliver, J. Gwyther, G. R. Whittell, I. Manners, *Chem. Soc. Rev.* **2016**, *45*, 5358.
- [23] R. A. Musgrave, A. D. Russell, I. Manners, *Organometallics* **2013**, *32*, 5654.
- [24] M. Gallei, S. Tockner, R. Klein, M. Rehahn, *Macromol. Rapid Commun.* **2010**, *31*, 889.
- [25] C. Tonhauser, M. Mazurowski, M. Rehahn, M. Gallei, H. Frey, *Macromolecules* **2012**, *45*, 3409.
- [26] M. Mazurowski, M. Gallei, J. Li, H. Didzoleit, B. Stühn, M. Rehahn, *Macromolecules* **2012**, *45*, 8970.
- [27] P. F. Eiland, R. Pepinsky, *J. Am. Chem. Soc.* **1952**, *74*, 4971.
- [28] J. D. Dunitz, L. E. Orgel, A. Rich, *Acta Cryst.* **1956**, *9*, 373.
- [29] F. Takusagawa, T. F. Koetzle, *Acta Crystallogr., Sect. B: Struct. Sci. Cryst. Eng. Mater.* **1979**, *B35*, 1074.
- [30] M. S. Inkpen, S. Scheerer, M. Linseis, A. J. White, R. F. Winter, T. Albrecht, N. J. Long, *Nat. Chem.* **2016**, *8*, 825.
- [31] C. Rüttiger, V. Pfeifer, V. Rittscher, D. Stock, D. Scheid, S. Vowinkel, F. Roth, H. Didzoleit, B. Stühn, J. Elbert, E. Ionescu, M. Gallei, *Polym. Chem.* **2016**, *7*, 1129.
- [32] D. Scheid, G. Cherkashinin, E. Ionescu, M. Gallei, *Langmuir* **2014**, *30*, 1204.
- [33] G. Mera, M. Gallei, S. Bernard, E. Ionescu, *Nanomaterials* **2015**, *5*, 468.
- [34] P. Nguyen, P. Gómez-Elipe, I. Manners, *Chem. Rev.* **1999**, *88*, 1515.
- [35] G. Masson, P. Beyer, P. W. Cyr, A. J. Lough, I. Manners, *Macromolecules* **2006**, *39*, 3720.
- [36] G. E. Southard, M. D. Curtis, *Organometallics* **2001**, *20*, 508.
- [37] G. R. Fulmer, A. J. M. Miller, N. H. Sherden, H. E. Gottlieb, A. Nudelman, B. M. Stoltz, J. E. Bercaw, K. I. Goldberg, *Organometallics* **2010**, *29*, 2176.
- [38] G. Sheldrick, *Acta Crystallogr., Sect. A: Found. Adv.* **2008**, *64*, 112.
- [39] S. Liu, A. M. Invergo, J. P. McInnis, A. R. Mouat, A. Motta, T. L. Lohr, M. Delferro, T. J. Marks, *Organometallics* **2017**, *36*, 4403.
- [40] L. Wirtz, W. Haider, V. Huch, M. Zimmer, A. Schäfer, *Chem. - Eur. J.* **2020**, *26*, 6176.
- [41] D. A. Foucher, R. Ziembinski, B. Z. Tang, P. M. Macdonald, J. Massey, C. R. Jaeger, G. J. Vancso, I. Manners, *Macromolecules* **1993**, *26*, 2878.
- [42] W. Finckh, B. Z. Tang, D. A. Foucher, D. B. Zamble, R. Ziembinski, A. Lough, I. Manners, *Organometallics* **1993**, *12*, 823.
- [43] J. Elbert, H. Didzoleit, C. Fasel, E. Ionescu, R. Riedel, B. Stühn, M. Gallei, *Macromol. Rapid Commun.* **2015**, *36*, 597.